Analyst

COMMUNICATION

Cite this: *Analyst*, 2014, **139**, 5660

Received 23rd July 2014
Accepted 11th September 2014

DOI: 10.1039/c4an01342e

www.rsc.org/analyst

Rituximab–Au nanoprobes for simultaneous dark-field imaging and DAB staining of CD20 over-expressed on Raji cells†

Lin Fan,‡[a] Doudou Lou,‡[a] Yu Zhang*[a] and Ning Gu*[b]

A novel dual-modal cell immunodetection method based on both dark-field imaging and catalysis functions of gold nanoparticles has been established, where the Rituximab–Au conjugates were used as nanoprobes to label and image specifically the CD20 overexpressed on the surface of malignant lymphoma cells of Raji with high affinity.

With the development of nanotechnology, gold nanoparticles exhibit high potential in tumor inhibition,[1] thermotherapy,[2] and diagnosis[3,4] because of their special optical[5] and electrical properties,[6] good stability and surface effects,[7] as well as the special size-dependent[8] biological compatibility and limited cytotoxicity.[9,10] El-Sayed *et al.* reported the applications of gold nanorods in both molecular imaging and photothermal cancer therapy.[11] Compared with other shapes, nanorods had longer circulation time in the blood, and higher accumulation in the tumour.[12] In their work, nanorods were modified with antibodies, in order to bind specifically to the surface of malignant cells. As a result of the scattered light from gold nanorods in the dark-field, the malignant cells were visualized and diagnosed from the normal ones. Furthermore, the malignant cells can be selectively destroyed using a low-energy harmless near-infrared laser without harming the surrounding nonmalignant cells. In Hu's work,[13] specific biomolecule functionalized gold nanorods and silver nanoparticles were used as probes for multiplex dark-field targeted imaging of pancreatic cancer cells due to their widely separated localized plasmon resonance characteristics. Raschke *et al.*[14] also proposed a method for biomolecular recognition using light scattering of a single gold nanoparticle coated with streptavidin, where a spectral shift of the functionalized gold nanoparticle plasmon resonance was induced by specifically combining with biotinylated molecules due to the alteration of the dielectric environment around gold nanoparticles.

Recently, gold nanoparticles have become a mimic enzyme research focus, not only because of their catalytic activities but also because they avoid the disadvantages of natural enzymes. He and coworkers[15] demonstrated that gold nanorods coated with a shell composed of Pt nanodots exhibited intrinsic oxidase-like, peroxidase-like and catalase-like activity, which was evaluated using the typical horse radish peroxidase (HRP) substrates such as 3,3,5,5-tetramethylbenzidine (TMB) and *O*-phenylenediamine (OPD) in the presence of H_2O_2. These new enzyme nanomimetics have competitive advantages in aspects of cost, preparation technology, stability and catalytic activity, and have been applied in bioanalysis instead of HRP, including detection of H_2O_2, glucose, and proteins.[15,16]

The fluorescence *in situ* hybridization (FISH) method[17] and immune histochemical (IHC)[18] technique have become the most common tools in cancer detection. The immunohistochemical technique is simple and low-cost, however, it cannot realize quantitatively detection and relies too heavily on the experiences and subjective judgment to ensure accuracy. For the FISH method, which though can realize accurate quantitative detection, the promotion and application were hindered by the high cost. Here a novel dual-modal cell immunodetection method was proposed, which combined both quantitative and low-cost advantages by using gold nanoparticles as probes to dark-field imaging and 3,3′-diaminobenzidin (DAB) staining of cancer cell membrane molecules. And the two imaging modalities were combined to gain more reliable information in a single picture. The integration of dark-field and bright field imaging modes in the same microscope greatly reduces the cost and improves the speed to get a dual-mode image with a simple switch. Compared with traditional immune cell imaging which

[a]*State Key Laboratory of Bioelectronics, Jiangsu Key Laboratory for Biomaterials and Devices, School of Biological Science and Medical Engineering, Southeast University, Nanjing, P. R. China. E-mail: zhangyu@seu.edu.cn; Fax: +86 25 8327 2496; Tel: +86 25 8327 2496*

[b]*State Key Laboratory of Bioelectronics, Jiangsu Key Laboratory for Biomaterials and Devices, School of Biological Science and Medical Engineering, Southeast University, Nanjing, P. R. China. E-mail: guning@seu.edu.cn; Fax: +86 25 8327 2496; Tel: +86 25 8327 2496*

† Electronic supplementary information (ESI) available: Experimental details, size distribution histograms, electron diffraction patterns, and Raman spectra. See DOI: 10.1039/c4an01342e

‡ These authors contributed equally to this work.

This journal is © The Royal Society of Chemistry 2014

uses natural horse radish peroxidase (HRP) to catalyze the chromogenic reaction of substrates, gold nanoparticles as mimetic peroxidase are low cost and easy to be prepared and combined to the antibody. At the same time, the dark-field imaging specifically comes from the light scattering of gold nanoparticles, avoiding the negative effect of endogenous enzymes to the catalytic process and the misjudgment resulting from the substrate instability in the bright field imaging. The complementation of the two modes can greatly increase the accuracy.

We employed gold nanoparticles to prepare the Rituximab–Au nanoprobes. The gold nanoparticles with good dispersity as well as the corresponding nanoprobes were evaluated by transmission electron microscopy (TEM) (Fig. S1, ESI†), UV-vis spectroscopy and dynamic light scattering (DLS) (Fig. S2 and S3, ESI†). The average diameter and hydrodynamic size of bared gold nanoparticles were about 10.0 nm and 16.7 nm, respectively. Rituximab, a commercial therapeutic antibody with CD20 specificity, was used to construct nanoprobes. After conjugating the gold nanoparticles with the Rituximab antibody, the hydrodynamic size increased significantly to 63.6 nm, while the TEM size remained unchanged almost. And as measured by using the BCA kit, the coupling efficiency of Rituximab on gold nanoparticles was 57.6% and the average number of antibodies on a single nanoparticle was about 7.5.

Malignant lymphoma cells of Raji (with CD20 overexpression) and leukemia cells of K562 (without CD20 overexpression) were used to make smears on microscope slides followed by immobilization with polyformaldehyde, and then incubated with the Rituximab–Au nanoprobes.

We installed an experimental group and five control groups to study the specificity of the detection (Schemes 1 and S1, ESI†). Cells were treated as described below and then observed under both bright-field and dark-field microscopes. The light scattering images were adjusted to a uniform background using Photoshop 8.0.1 (Fig. S4, ESI†). In the experimental group, Raji cells were incubated with the Rituximab–Au nanoprobes at 37 °C for 1 hour and washed with 1% PBS-T three times to remove the redundant nanoprobes (Scheme 1). As a result, the nanoprobes were specifically bound to the overexpressed CD20 on the surface of Raji cells, and the strong scattering light from the Rituximab–Au nanoprobes on the cell membrane was clearly observed in the dark-field as expected, with a low non-specific binding rate (Fig. 1a). The gold nanoparticles without protein coating were also employed as the gold nanoparticle group instead of the Rituximab–Au nanoprobes (Scheme S1a, ESI†). In this group, lots of gold nanoparticles were deposited on the surface of cells non-specifically and irregularly due to the lack of the protection of antibodies and BSA blocking (Fig. 1e).

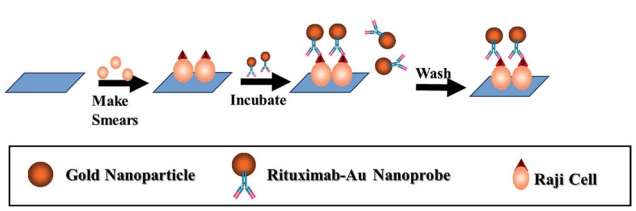

Scheme 1 Labelling process of the Rituximab–Au nanoprobes for CD20 over-expressed Raji cells.

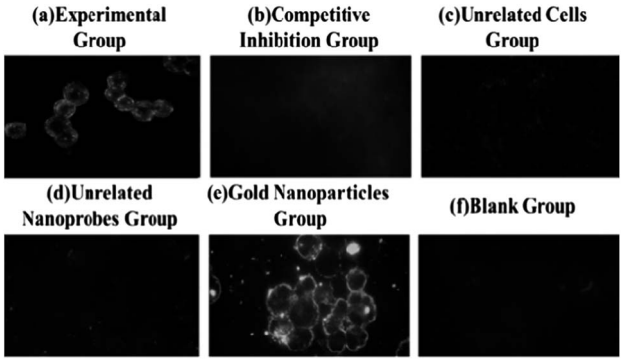

Fig. 1 Dark-field images of Raji cells labelled by the Rituximab–Au nanoprobes for the experimental group (a). Other dark-field images for five control groups (b)–(f) were also described as noted in the figure. All images were adjusted to a uniform background colour by using image manipulation software of Photoshop 8.0.1.

In the competitive inhibition group, Raji cells' binding sites were blocked by 100 times the amount of Rituximab monoclonal antibodies before incubating with the Rituximab–Au nanoprobes (Scheme S1b, ESI†). For the unrelated cell group and the unrelated nanoprobe group, we changed the cells and the probes to K562 cells (without CD20 overexpress) and human IgG–Au nanoprobes respectively (Scheme S1c and d, ESI†). And in the blank group, Raji cells were co-incubated with the buffer of PBS-T instead of gold nanoprobes (Scheme S1e, ESI†). As a result, the four group cells could not be successfully labelled and thus hardly be observed in the dark-field (Fig. 1b–d and f).

Note that the bright-field images did not show regularity under different experimental conditions (Fig. S5, ESI†). As fixed with 4% paraformaldehyde to make smears, the Raji cells have been killed already and lost the effects of cellular endocytosis before co-incubating with Rituximab–Au nanoprobes. It is proved that the difference among six groups was due to light-scattering of gold nanoprobes labelled on the surface of the cells rather than the cells themselves or non-specific adsorption. This provided evidence that the scattering intensity reflected the gold nanoparticle bonding situation on the surface of cells.

We installed four inhibition groups by antibody blocking to indirectly study the correspondence between the amount of gold nanoparticles adsorbed on the cell surface and the expression levels of CD20. In the four groups, Raji cells' binding sites (CD20) were blocked by 100 (Fig. 2a), 50 (Fig. 2b), and 10 (Fig. 2c) times the amount of Rituximab monoclonal antibodies and PBS-T (Fig. 2d) before incubating with the Rituximab–Au nanoprobes. With decreasing the amount of Rituximab, the scattering intensity revealed a linear increasing trend due to the increase of effective binding sites of Raji cells. Furthermore, we compared the dark-field (Fig. S6a, ESI†) and the bright field (Fig. S6b, ESI†) images in the same visual field and found that almost 100% cells can be labelled by Rituximab–Au nanoprobes.

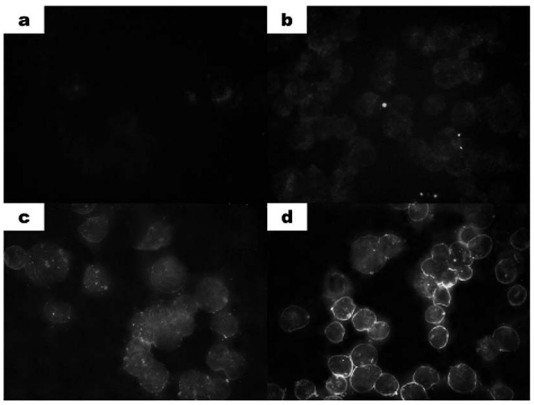

Fig. 2 Dark-field images of Raji cells when CD20 binding sites blocked by 100 (a), 50 (b), and 10 (c) times and, (d) without Rituximab respectively.

Besides that, we used gold nanoparticles as mimetic peroxidase to catalyse colour reaction with DAB as a chromogenic substrate in the presence of hydrogen peroxide. Due to the specific binding of the Rituximab–Au nanoprobes on the cells, Raji cells were stained brown by DAB deposition reaction, as observed in the bright-field (Fig. 3a). The degree of DAB staining reaction could reflect the amount of the bound nanoprobes on the cells, that is, the degree of the CD20 over-expression. For comparison, cells labelled with the Rituximab–Au nanoprobes but not stained with DAB were clear and colourless in the bright-field (Fig. 3b). By comparing the corresponding dark-field images (Fig. 3c and d), we found that higher-contrast images of the dark-field could also be obtained by DAB deposition reaction, likely due to the enhanced scatter from DAB deposition.

The non-specific binding decrease plays an important role in improving the specificity and accuracy of tumour detection methods. The Rituximab–Au nanoprobes purified by centrifugation could be completely resuspended in citrate buffer containing 1% BSA or 0.2% PEG20000. BSA was used to block

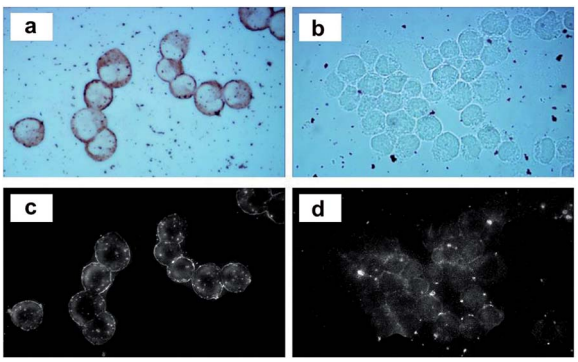

Fig. 3 (a) Bright-field image of Raji cells when labelled with the Rituximab–Au nanoprobes which acted as peroxidase to catalyse the colour reaction of DAB. (b) Bright-field image of Raji cells with Rituximab–Au nanoprobes labelling but without DAB staining. (c and d) The dark-field images corresponding to (a) and (b), respectively.

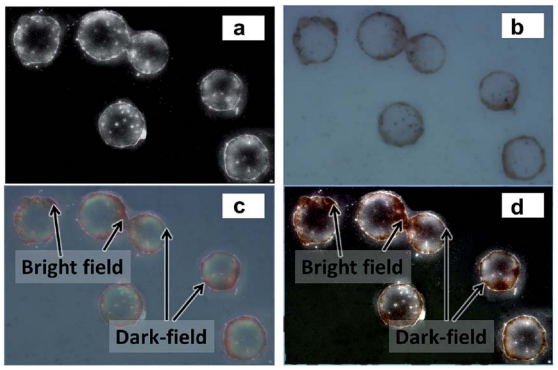

Fig. 4 Combination of bright-field image and dark-field image. (a) Dark-field image of Raji cells when labelled with the Rituximab–Au nanoprobes; (b) bright-field image of Raji cells when labelled with the Rituximab–Au nanoprobes and stained with DAB; (c) overlap the two images (a) and (b) and adjust the opacity; (d) adjust the clarity of the processed images.

residual binding sites on the gold nanoparticle surface, while PEG20000 was used to decrease the non-specific adsorption[19] (Fig. S7a and f, ESI†). Gold nanoprobe aggregates easily formed during the centrifugal purification and deposited on the surface of smears, which enhanced non-specific binding. This could be solved by short-time low-speed centrifugation (Fig. S7f and g, ESI†). In addition, dipping slides in PBS-T solution was also useful for decreasing non-specific adsorption (Fig. S7f and h, ESI†). With incubating time prolonging, both specific and non-specific binding amounts enhanced, so an optimized incubation time of 60 min was selected, which was proved to be able to harvest very weak nonspecific binding (Fig. S7b, c and f, ESI†). The concentration affected both labeling effects and stability of the nanoprobes. Compared with 57.9 μg ml^{-1} (Fig. S7d, ESI†) and 115.8 μg ml^{-1} (Fig. S7e, ESI†), an optimized nanoprobe concentration of 289.5 μg ml^{-1} (OD value of 4.3 at 560 nm) (Fig. S7f, ESI†) of gold nanoparticles significantly increased the detection sensitivity without leading to the non-specific adsorption and nanoprobe aggregation.

In order to gain complementary information in a single picture and achieve more reliable detection results, we overlapped the two images and adjusted the opacity and the clarity of the processed image. In the processed image, we can see that Raji cells were stained brown by DAB in the bright-field and shown as yellow-white bright circles in the dark-field, which could both reflect the amount of the bound nanoprobes on the cells (Fig. 4).

Conclusions

We provide an *in vitro* detection method using Rituximab–Au nanoprobes as novel contrast agents for cell imaging in both the bright-field and dark-field. The Rituximab–Au nanoprobes bind specifically to the surface of Raji cells due to the overexpressed CD20. As a result of the strongly scattered light from gold nanoparticles, the over-expression rate of CD20 is positively correlated with the luminosity of the cells in the dark-field. And

This journal is © The Royal Society of Chemistry 2014

in the bright-field, the expression level of CD20 can also be reflected by the degree of DAB staining catalyzed by gold nanoparticles with peroxidase-like activity. We combine the two images, in order to gain more reliable information in a single picture. As the scattering intensity can be quantified, there is a reason to expect to be able to establish quantificational detection of cell-surface molecules based on gold nanoprobes scattering in the dark-field. Relevant software for measuring scattering intensity is under development.

Acknowledgements

This research was supported by the National Important Science Research Program of China (no. 2011CB933503 and 2013CB733800), the National Natural Science Foundation of China (no. 31170959), the Basic Research Program of Jiangsu Province (Natural Science Foundation, no. BK2011036), the Jiangsu Provincial Technical Innovation Fund for Scientific and Technological Enterprises (no. SBC201310643) and the National Key Technology Research and Development Program of the Ministry of Science and Technology of China (no. 2012BAI23B02).

Notes and references

1 C. O. Tetteym, P. C. Nagajyothi, S. E. Lee, *et al.*, Anti-melanoma, tyrosinase inhibitory and anti-microbial activities of gold nanoparticles synthesized from aqueous leaf extracts of *Teraxacum officinale*, *Int. J. Cosmet. Sci.*, 2012, **34**, 150–154.

2 L. B. Carpin, L. R. Bickford, G. Agollah, *et al.*, Immunoconjugated gold nanoshell-mediated photothermal ablation of trastuzumab-resistant breast cancer cells, *Breast Cancer Res. Treat.*, 2011, **125**, 27–34.

3 K. K. Jain, Advances in the field of nanooncology, *BMC Med.*, 2010, **8**, 83.

4 J. F. Hainfeld, M. J. O'Connor, F. A. Dilmanan, *et al.*, Micro-CT enables microlocalisation and quantification of Her2-targeted gold nanoparticles within tumour regions, *Br. J. Radiol.*, 2011, **6**(84), 526–533.

5 S.-K. Baek, A. R. Makkouk, T. Krasieva, *et al.*, Photothermal treatment of glioma; an in vitro study of macrophage-mediated delivery of gold nanoshells, *J. Neuro-Oncol.*, 2011, **104**(2), 439–448.

6 S. Jain, D. G. Hirst and J. M. O'sullivan, Gold nanoparticles as novel agents for cancer therapy, *Br. J. Radiol.*, 2012, **85**, 101–113.

7 R. Arvizo, R. Bhattacharya and P. Mukherjee, Gold nanoparticles: Opportunities and Challenges in Nanomedicine, *Expert Opin. Drug Delivery*, 2010, **7**(6), 753–763.

8 K. Huang, H. Ma, J. Liu, *et al.*, Size-Dependent Localization and Penetration of Ultrasmall Gold Nanoparticles in Cancer Cells, Multicellular Spheroids, and Tumors in Vivo, *ACS Nano*, 2012, **6**(5), 4483–4493.

9 K. T. Butterworth, J. A. Coulter, S. Jain, *et al.*, Evaluation of cytotoxicity and radiation enhancement using 1.9 nm gold particles: potential application for cancer therapy, *Nanotechnology*, 2010, **21**(29), 295101.

10 A. M. Alkilany and C. J. Murphy, Toxicity and cellular uptake of gold nanoparticles: what we have learned so far?, *J. Nanopart. Res.*, 2010, **12**, 2313–2333.

11 P. K. Jain, I. H. El-Sayed and M. A. El-Sayed, Au nanoparticles target cancer, *Nano Today*, 2007, **2**(1), 18–29.

12 Arnida, M. M. Janát-Amsbury, A. Ray, *et al.*, Geometry and Surface Characteristics of Gold Nanoparticles Influence their Biodistribution and Uptake by Macrophages, *Eur. J. Pharm. Biopharm.*, 2011, **77**(3), 417–423.

13 R. Hu, K. T. Yong, I. Roy, *et al.*, Metallic nanostructures as localized plasmon resonance enhanced scattering probes for multiplex dark-field targeted imaging of cancer cells, *J. Phys. Chem. C*, 2009, **113**(7), 2676–2684.

14 G. Raschke, S. Kowarik, T. Franzl, *et al.*, Biomolecular recognition based on single gold nanoparticle light scattering, *Nano Lett.*, 2003, **3**(7), 935–938.

15 W. He, Y. Liu, J. Yuan, *et al.*, Au@Pt nanostructures as oxidase and peroxidase mimetics for use in immunoassays, *Biomaterials*, 2011, **32**(4), 1139–1147.

16 Y. Jv, B. Li and R. Cao, Positively-charged gold nanoparticles as peroxidiase mimic and their application in hydrogen peroxide and glucose detection, *Chem. Commun.*, 2010, **46**(42), 8017–8019.

17 S. Weremowicz, D. J. Sandstrom and C. C. Morton, *et a1.*, Fluorescence in situ hybridization (FISH) for rapid detection of aneuploidy: experience in 911 prenatal cases, *Prenatal Diagn.*, 2001, **21**(4), 262–269.

18 R. Tanaka, T. Yuhi and N. Nagatani, *et a1.*, A novel enhancement assay for immunochro-matographic test strips using gold nanoparticles, *Anal. Bioanal. Chem.*, 2006, **385**, 1414–1420.

19 M. Bartneck, H. A. Keul and S. Singh, *et a1.*, Rapid Uptake of Gold Nanorods by Primary Human Blood Phagocytes and Immunomodulatory Effects of Surface Chemistry, *ACS Nano*, 2010, **4**(6), 3073–3086.